

# Geo-Spatial Analysis of Aarey Colony subregion, Mumbai: LULC Classification Using Machine-Learning

<sup>1</sup>Ayan Shaikh, <sup>2</sup>Vighnesh Shinde, <sup>3</sup>Atharv Rane, <sup>4</sup>Devanand Bathe

<sup>1</sup>Student, <sup>2</sup>Student, <sup>3</sup>Student, <sup>4</sup>Assistant Professor

<sup>1</sup>Department of Artificial Intelligence and Data Science,

<sup>1</sup>KJ Somaiya Institute of Technology, Mumbai, India

[ayan12@somaiya.edu](mailto:ayan12@somaiya.edu), [vighnesh13@somaiya.edu](mailto:vighnesh13@somaiya.edu), [atharv.rane@somaiya.edu](mailto:atharv.rane@somaiya.edu),  
[devanandkb@somaiya.edu](mailto:devanandkb@somaiya.edu)

**Abstract**—Geo-spatial data or geodata refers to data or information related to geographical locations on the Earth's surface and includes vectors, attributes, and raster and satellite imagery. Remote sensing serves as one of the primary sources for generating geospatial information like satellite images. The analysis of spatial information is an important area of research due to its wide variety of applications such as urban planning, Land Use and Land Cover (LULC) classification, agriculture, environmental monitoring, deforestation tracking, etc. Since its launch in 2013, Landsat-8 has played a key role in such analyses. This paper focuses on a specific land survey of Aarey Colony, aiming to classify and analyze its Land Use and Land Cover (LULC) using satellite imagery from Landsat-8. The research emphasizes combining geospatial data with advanced Python tools and machine learning algorithms to distinguish between natural and artificial land covers. By leveraging Python libraries like GeoPandas, Rasterio, and Scikit-learn, along with the Google Earth Engine API, this study seeks to present a detailed understanding of the spatial dynamics of Aarey Colony.

**Index Terms**—Geo-spatial data, Python, Rasterio, Satellite imagery, Machine learning, Remote Sensing, Aarey Colony.

## I. INTRODUCTION

Geo-spatial data refers to information associated with specific locations and geographic features of the Earth. It is widely used in various domains due to its ability to provide spatial context to information. This data type includes coordinates, addresses, complex geographic shapes, raster data and satellite images. Python is one of the most widely used programming languages for remote sensing and geospatial analysis applications. Due to its versatility, ability to install, import, and run various packages and adaptability, Python is a popular choice for image segmentation, which is one of the key pre-processing techniques used in the analysis of Earth data. GIS (Geographic Information System) software, like ArcGIS and QGIS, which are used to modify, analyze, and store geospatial data, are also written and developed in Python. In this paper, we focus on the collection of satellite images, their manipulation, preprocessing and analysis using Python libraries. This study makes use of Python in the location-specific context of Aarey Colony, - a forested sub locality of Mumbai, India - leveraging major geodata manipulation libraries in Python such as GDAL and Rasterio. The study encompasses main techniques in spatial data processing, analysis, and visualization, particularly in the classification and understanding of Land Use and Land Cover (LULC) within the region. A time series analysis monitors LULC trends based on spectral indices over time in Aarey Colony with the aim of unearthing insights into environmental changes.

## II. BACKGROUND

### A. Types of Geo-spatial Data Vector data

This denotes distinct objects like points, lines and polygons i.e., it has a coordinate-based structure. Such objects are commonly used for mapping urban features like roads, buildings, and boundaries (edges). Common formats of vector spatial data include GeoJSON and PostGIS. Raster data: This type of spatial data represents continuous data like satellite imagery, represented in the form of a grid consisting of pixels arranged in rows and columns. The widely used raster data formats are GeoTIFF, JPEG, and PNG. Due to high resolution, the file size for these formats is large.

### B. Data Sources

The development of free and open-source platforms for satellite images like Sentinel (by European Space Agency) and USGS i.e. United States Geological Survey has played a vital role in research advancements in remote sensing and acquisition of spatial data [2]. These platforms provide enhanced accessibility of geographic information and resources without the high costs involved in commercial data sourcing. • LANDSAT - 8: Established in February 2013, the LANDSAT - 8 satellite is operated by the United States Geological Survey and is part of the Landsat program. Its primary purpose is to provide earth observation data [9]. Its spatial resolution is 30m for visible reflectance and infrared bands. Landsat-8 is equipped with two key instruments—the Operational Land Imager (OLI) and the Thermal Infrared Sensor (TIRS)—that capture detailed images of the Earth surface [14]. OLI captures information across nine spectral bands, ranging from visible light to shortwave infrared, while TIRS collects data in two thermal bands, which are particularly useful for studying surface temperatures [3]. These sensors facilitate precise LULC classification by capturing data at different wavelengths and resolutions, making Landsat-8 ideal for analyzing varied land features such as water bodies, forests, urban areas, and agricultural zones. • Sentinel Hub: The Sentinel Hub was launched by the European Space Agency (ESA) as part of its Copernicus Program and consists of Sentinel -1, Sentinel -2, Sentinel -3, Sentinel -5P satellites. The purpose of the Copernicus Program is to provide free access to satellite images or data captured by the Sentinel Hub satellites. Sentinel -2 provides a spatial resolution of 10m for visible and NIR bands, and 20m

for SWIR bands. The satellite images obtained from such open-source platforms play a key role in facilitating data collection for research, observation and analysis purposes • Google Earth Engine (GEE): GEE is a cloud-based platform designed for geospatial analysis, combining a massive collection of satellite imagery and spatial data with strong computing capabilities to process and analyze it efficiently [8]. Developed by Google, it enables researchers to access, process, and analyze large-scale geospatial and raster data efficiently without requiring local storage or computational resources. GEE offers preprocessed datasets (e.g., surface reflectance, TOA) which are crucial for analysis without additional preprocessing steps. It is most widely used for time-series analysis and machine learning-based classification, offering a range of specialized algorithms, geometric and ML capabilities [8].

### C. Remote Sensing Overview

Remote sensing involves gathering information about the Earth's surface without needing to physically touch it, typically done using sensors mounted on satellites or aircraft, which capture data from a distance [20]. These sensors capture the different wavelengths of light emitted by geographic features like mountains, lakes, seas, oceans, forests, etc. and urban features like roads, buildings, towers, and so on. This data is then used to monitor environmental changes and provide useful insights into land use and land cover (LULC), and urban planning [19][20]. Remote sensing captures data over large and inaccessible areas, providing comprehensive coverage that would be difficult to obtain otherwise. Remote sensing can be done in the following 2 ways: 1. Active sensing: Active sensing makes use of sensors that generate their own light source to observe objects. These sensors emit radiation toward the object under study and subsequently detect and measure the radiation that is reflected back from the target [10]. 2. Passive sensing: Passive sensors measure the natural energy, such as radiation, that is either emitted or reflected by the target or scene. The most frequent source of radiation captured by passive sensors is reflected sunlight [10].

## III. REVIEW OF PYTHON LIBRARIES FOR GEO-SPATIAL ANALYSIS

### A. GDAL

The Geospatial Data Abstraction Library (GDAL) is an open-source library designed for reading and writing both raster and vector spatial data formats, such as Shapefile and GeoTIFF. GDAL is a popular approach to addressing the analysis and manipulation of the diversity of raster and vector data formats. It is used extensively in Geographic Information System (GIS) software like QGIS and GRASS GIS for data pre-processing and storage. According to Lemenkova and Debeir (2023), 'the major advantage of the GRASS GIS, similar to the QGIS, is that it combines the GUI with command-line interface (CLI) run from the console and enables operation with cartographic projections by GDAL'. GDAL has robust capabilities for reprojecting geospatial data between different coordinate reference systems, transforming data to match specific map projections and spatial resolutions.

### B. Rasterio

Rasterio is a Python library used for working with raster data which makes it highly significant for working with satellite imagery, DEMs, and other grid-based data. It provides tools for reading raster formats (e.g., GeoTIFF) [8], reprojecting images, clipping data based on vector shapes and performing pixel calculations. Rasterio integrates well with the NumPy package for raster data manipulation and Pandas package for data analysis. It is commonly used in environmental monitoring and land cover classification. Due to its ability to integrate smoothly with Pandas and NumPy for calculations, a common application of Rasterio is to calculate vegetation indices like NDVI and SAVI [9].

### C. EarthPy

EarthPy is a Python package which is built on top of other geospatial software libraries like Rasterio, Geopandas and Matplotlib [9]. EarthPy simplifies the visualization of Earth observation data, mainly raster and remote sensing data obtained from satellites. According to Wasser, Joseph and Head (2019), 'EarthPy makes commonly performed spatial data exploration tasks easier for scientists by building upon functions in the widely used packages: Rasterio and GeoPandas. EarthPy is designed for users who are new to Python and spatial data with a focus on scientific data.' It was originally developed as an educational tool at Earth Lab - University of Colorado (Wasser et al. 2019)

## IV. METHODOLOGY

### A. Study Area

Aarey Colony is located at 19° 08' 54.57" N and 72° 52' 54.32" E, in the northern suburbs of Goregaon (East), Mumbai, India. It is a sprawling urban forest covering approximately 1,300 hectares. Established in 1949, it is a critical green belt in Mumbai, often called the "lungs of the city." Home to over 290 species of flora and fauna, including rare and endangered species, it plays a vital role in maintaining biodiversity and ecological balance. However, Aarey faces growing threats from urbanization and deforestation due to projects like metro car sheds and residential developments. These activities have reduced forest cover, disrupted wildlife habitats, and diminished essential ecosystem services such as air purification and temperature regulation.



Fig. 1. An overview of Landsat-8's global land coverage capacity and spectral bands

## B. Data Acquisition

In this study, high resolution LANDSAT - 8 satellite images are obtained from Google Earth Engine. GEE code editor allows users to manually select the coordinates in order to retrieve high-resolution geospatial data. Landsat-8 data is made freely available by the United States Geological Survey and GEE allows access to Landsat-8 data [14]. The dataset used for training the Random Forest Classifier and ResNet18 Deep Neural Network comprised of 300 LANDSAT - 8 multispectral images (150 images corresponding to Bands 2, 3 and 4, and 150 images corresponding to Bands 4, 5 and 6) with spectral bands obtained from the USGS archive Landsat 8 Operational Land Imager (OLI) and Google Earth Engine. Specific spectral bands of the GeoTIFF images are used in the calculation of spectral indices such as Normalized Difference Vegetation Index (NDVI), Normalized Difference Moisture Index (NDMI) and Normalized Difference Built-up Index (NDBI) which are used for differentiating the dataset into classes. For the spatio-temporal and LULC change analysis of Aarey Colony, this study utilizes 12 years of satellite imagery data of the Aarey forest area, comprising 64 images captured using spectral Bands 2, 3, 4 and Bands 4, 5, 6, with three images per year. For each year, the first image corresponds to the January–May period, the second to October–November, and the third to December.

## C. Calculation of Spectral Indices

Spectral indices are mathematical formulas that use the reflectance values from different satellite bands to emphasize certain features of the Earth's surface. They help make raw satellite data easier to understand and analyze. In this study, three key indices were calculated: the Normalized Difference Vegetation Index (NDVI), the Normalized Difference Moisture Index (NDMI), and the Normalized Difference Built-up Index (NDBI).

1) Normalized Difference Vegetation Index (NDVI): The Normalized Difference Vegetation Index (NDVI) is a widely used metric for quantifying vegetation health and density [9]. It exploits the high reflectance of vegetation in the Near Infrared (NIR) spectrum and the strong absorption of red light due to chlorophyll. NDVI values lie between -1 to +1. Higher or more positive values indicate healthy and dense vegetation while lower or negative values indicate barren land, water or urban settlements [7].

$$\text{NDVI} = \frac{\text{NIR} - \text{Red}}{\text{NIR} + \text{Red}}$$

Where: • **NIR** = Near Infrared reflectance (Band 5) • **Red** = Red band reflectance (Band 4)

2) Normalized Difference Moisture Index (NDMI): NDMI is primarily used to evaluate vegetation moisture content and helps to detect drought conditions. It contrasts the reflectance in the Near Infrared (NIR) and Shortwave Infrared (SWIR1) bands.

$$\text{NDMI} = \frac{\text{NIR} - \text{SWIR1}}{\text{NIR} + \text{SWIR1}}$$

Where: • **NIR** = Near Infrared reflectance (Band 5) • **SWIR1** = Shortwave Infrared reflectance (Band 6)

3) Normalized Difference Built-up Index (NDBI): NDBI distinguishes built-up areas from other kinds of land cover like vegetation, scrub, etc. Built-up surfaces typically have higher reflectance in the SWIR1 band and lower reflectance in the NIR band.

$$\text{NDBI} = \frac{\text{SWIR1} - \text{NIR}}{\text{SWIR1} + \text{NIR}}$$

Where: • **SWIR1** = Shortwave Infrared reflectance (Band 6) • **NIR** = Near Infrared reflectance (Band 5)

4) Normalized Difference Water Index (NDWI): The primary purpose of NDWI is to detect water bodies and monitor changes in water content in land features. It enhances characteristics of water by maximizing the reflectance of water in the green band. This makes it useful in delineating open water surfaces.

$$\text{NDWI} = \frac{\text{Green} - \text{NIR}}{\text{Green} + \text{NIR}}$$

Where: • **Green** = Green reflectance (Band 3) • **NIR** = Near Infrared reflectance (Band 5)

## D. LULC Classification

Land Use and Land Cover (LULC) classification involves identifying and categorizing areas of the Earth based on their physical characteristics and the patterns of their usage. Land cover refers to physical features or natural surface of the earth such as vegetation, water, or urban infrastructure while land use defines how the land is being utilized for human activities. In this study, multi-band satellite imagery from Landsat 8 was used, sourced from the USGS and Google Earth Engine. These images have a spatial resolution of 30 meters. LULC Classification in this study focuses on two main techniques: the Random Forest Classifier (supervised learning) and Convolution Neural Network (ResNet 18 deep neural network). 5 primary classes were identified for the LULC Classification. These were vegetation, Desert, wetlands, water bodies and buildings. Table 1 provides a brief description of the classes.

Sr. No.	Class	Description
1	Vegetation	Areas covered by trees, shrubs, and other green spaces
2	Desert	Areas that are exposed and lack significant vegetation cover such as plowed agriculture fields, eroded lands, or fallow terrain.
3	Water Bodies	Rivers, lakes, reservoirs, and other permanent water features
4	Wetlands	Transitional zones between terrestrial and aquatic ecosystems
5	Urban/Buildings	Built-up areas like residential, commercial and industrial zones

TABLE I LAND USE LAND COVER CLASSES

1) Random Forest: Random Forest is an ML algorithm for supervised classification, where multiple decision trees are constructed during training and their outputs are combined to enhance accuracy and minimize overfitting [10][18]. The model leveraged Landsat-8's multi-spectral bands (Visible, NIR, SWIR) along with the derived spectral indices NDVI, NDMI and NDBI to distinguish between the five LULC classes. A total of 300 preprocessed images were used. Missing band values were addressed through linear interpolation and spatial resampling to standardize all images to 30m spatial resolution. The RF classifier was configured with 300 decision trees to balance computational efficiency and model accuracy and Gini impurity criterion was used to split nodes. The train-test split was adjusted to 80-20 to ensure robust validation. Furthermore, data augmentation techniques such as random flips, rotations ( $\pm 20^\circ$ ) and random brightness/contrast adjustments were employed to extend the training dataset and avoid overfitting problems.

2) ResNet 18 network: ResNet-18 architecture is a deep convolutional neural network (CNN) with residual learning frameworks. It was employed for multispectral LULC classification to exploit spatial-contextual patterns in satellite images. The model's input layer was adjusted to handle six channels, matching the six Landsat-8 bands used in the training data—resulting in a 6-channel input tensor. Transfer learning was used by starting with weights pretrained on ImageNet, while the last three residual blocks of the model were finetuned to better capture geospatial features. Data augmentation techniques were applied to the training images. These included random flips (horizontal and vertical), rotations, brightness and contrast adjustments, and shift-scale-rotate transformations to improve model robustness. These augmentations were aimed at simulating variations in environmental conditions and improving model generalization.

## E. Time Series Analysis

The study utilized a 12-year (2013–2024) Landsat-8 satellite imagery dataset of the Aarey Forest region, comprising 64 multispectral images. Three images per year were acquired seasonally: one during January–May (dry season), one during October–November (post-monsoon), and one in December (winter), with separate collections for bands 2–4 (visible NIR) and bands 4–6 (NIR-SWIR). Imagery was sourced via Google Earth Engine (GEE) using a custom script within the GEE Code Editor, which enabled manual delineation of the study area, selection of spectral bands (2–4 and 4–6), and temporal filtering. Time series analysis was performed on the calculated spectral indices—NDVI, NDMI, and NDBI—to observe patterns and changes over time, both quarterly and annually. These trends were illustrated using line graphs for visualization. Seasonal Autoregressive Integrated Moving Average (SARIMA) model was subsequently applied to forecast index values for six future intervals (2023–2024), enabling prediction of land cover dynamics over a two-year horizon.

## V. ANALYSIS AND RESULTS

Python packages along with Google Colab GPU were used to train RF model and ResNet-18 neural network for LULC classification. Time-series analysis of the Aarey subregion also revealed changes in LULC based on observing the trends in spectral indices.

### A. Random Forest

RF classifier achieved an overall accuracy of 69.11%. The class-specific F1-scores varied from 0.71 for wetlands to 1 for water bodies. Wetlands exhibited the lowest precision (0.67) due to spectral overlap with vegetation in NIR bands. Water bodies exhibit perfect separation due to unique reflectance in the SWIR band. Table II shows the performance of the model in detail and displays performance metrics precision, recall, F1 score and support for all 5 LULC classes. The classification of buildings proved as the most challenging, with the lowest F1-score (0.59) due to a low recall (0.50), indicating

misclassification. Fig. 2. shows feature importance for the six input bands used in the RF classifier. It describes how each band contributed to the classification of LULC classes. The x-axis represents band index (1 to 6) and the y-axis represents importance score of each band. This quantifies how much each band contributed to reducing impurity across all decision trees in the RF model. Bands 5 and 6 have the highest importance scores (greater than 0.2 each) indicating that they played the main role in distinguishing between the LULC classes. These are the NIR (band 5) and SWIR (band 6) bands. Both bands are sensitive to vegetation moisture and urban structures.

Class	Precision	Recall	F1-Score	Support
Vegetation	0.64	0.78	0.70	9
Desert	0.88	0.88	0.88	8
Water Bodies	1.00	1.00	1.00	13
Wetlands	0.67	0.75	0.71	8
Buildings/Urban	0.71	0.50	0.59	10
<b>Accuracy</b>	0.79 (Samples = 48)			
<b>Macro average</b>	0.78	0.78	0.77	48
<b>Weighted average</b>	0.80	0.79	0.79	48

TABLE II CLASSIFICATION REPORT OF RANDOM FOREST CLASSIFIER FOR LULC CATEGORIES

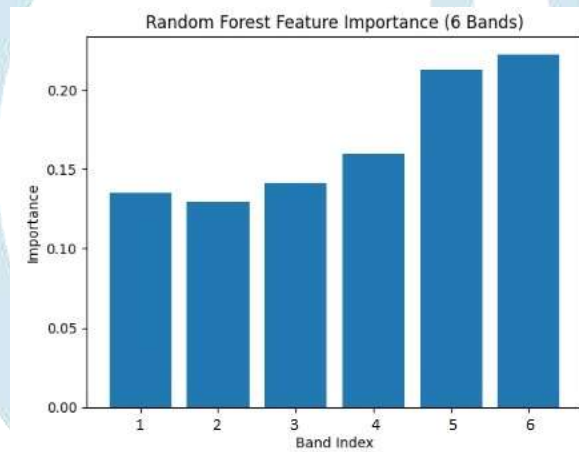


Fig. 2. Importance of each spectral band in the Random Forest Classifier

**B. Convolutional Neural Network (CNN) - ResNet 18**

ResNet-18 is a deep convolutional neural network architecture that introduces residual learning through “skip connections”, allowing the model to learn identity functions that help mitigate the vanishing gradient problem [11]. It contains 18 layers, including convolutional, batch normalization, ReLU activation and fully connected layers [17]. ResNet-18 achieved validation Accuracy of 95%. However, its computational demand (2 hours training on CPU vs. 5 minutes GPU runtime) and “black-box” nature posed trade-offs between accuracy and interpretability.

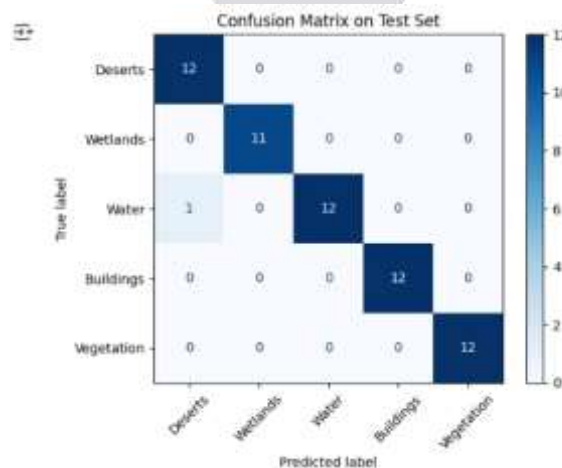


Fig. 3. Confusion matrix of RF for LULC classes

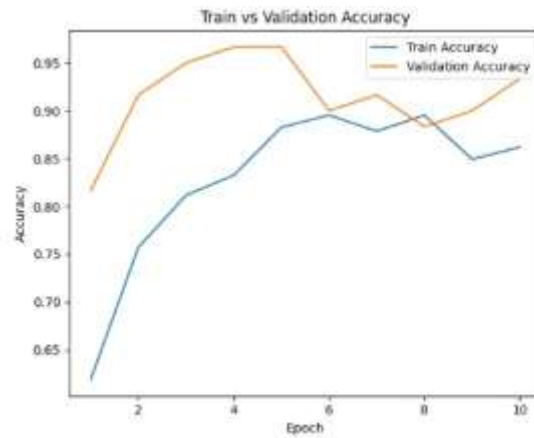
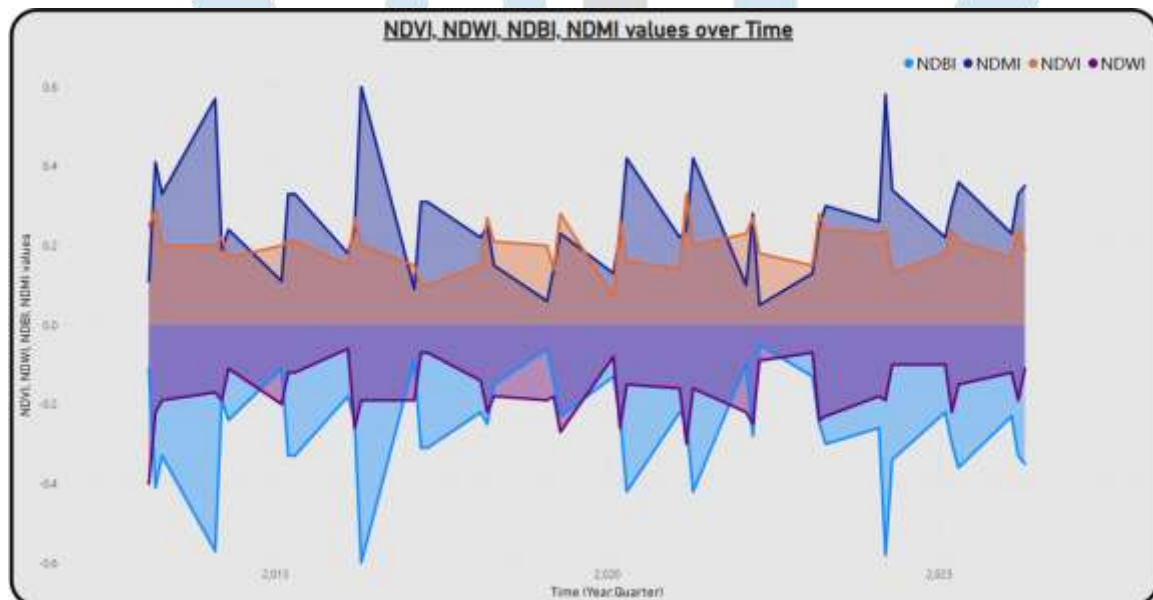


Fig. 4. Training vs. Validation Accuracy across 10 epochs for ResNet18 model. Plot illustrates the model's learning progression and performance during training

### C. Time Series analysis and trends

This study analyzes temporal trends in NDVI, NDMI, NDWI and NDBI values across Aarey Colony, derived from multi-year preprocessed Landsat-8 imagery. These indices provide information about vegetation health and moisture levels, aiding in the detection of seasonal and long-term land cover changes. Trends indicate periodic NDVI drops during monsoons, potentially due to dense canopy shadowing, while NDMI spikes suggest increased surface moisture. These patterns correlate with natural climatic cycles and urban activity in the region. Additional analysis reveals a distinct decline in NDVI during monsoon months, suggesting potential canopy loss or increased shadowing due to dense vegetation cover.



## VI. CONCLUSION

This study highlights the critical role of geospatial analysis in understanding patterns of land use and land cover change within Aarey Colony. Utilizing Landsat-8 imagery and Python-based tools, the research identified Land Use and Land Cover trends in the Aarey Colony subregion by calculating spectral indices such as NDVI, NDMI, NDWI, and NDBI over a 12-year period. The NDVI values are observed to be decreasing over the years. Strong quarterly variations observed which suggests that NDVI values fluctuate significantly across seasons. After 2020, NDVI improved slightly and reached a small peak. While limitations such as data resolution and validation exist, the insights gained could assist in laying the foundations for urban planning and conservation strategies. By advancing the methodologies and addressing the outlined challenges, future research can further strengthen the case for sustainable management of urban forests like Aarey Colony.

## VII. FUTURE DIRECTIONS

Building on the findings of this study, several avenues for future research and action are identified: • Integration of high-resolution satellite data or aerial imagery can provide more precise insights into small-scale changes • Advanced DL methods like Convolutional Neural Networks can be explored to enhance the accuracy of land cover classification and change detection. • The temporal scope can be expanded via the use of older datasets, such as Landsat-5 and Landsat-7, alongside Landsat-8. This can offer a broader and more diverse dataset for carrying out comprehensive historical analysis of land use changes. • Conducting field surveys for ground truth verification could lead to improvement in the reliability of classifications achieved by LULC classification models.

## REFERENCES

- [1] Priyanka, T., Veeraiah, B., & Jogu, L.S. (2024). Terrain Analysis of Elements Using LISS-IV Satellite Image in Bhainsa Region, Northwestern Part of Nirmal District, Telangana State, India. *Asian Journal of Geographical Research*, 7(2), 107-122.
- [2] H. Singh and K. Singh "Analysis of land use and land cover dynamics and drivers of urban expansion in and around Imphal city, India, using geospatial and random forest techniques" *GeoJournal* (2024) 89:169 <https://doi.org/10.1007/s10708-024-11190-8>.
- [3] Saha, J., Ria, S.S., Sultana, J., Shima, U.A., Seyam, M.M.H., & Rahman, M.M. (2024). Assessing seasonal dynamics of land surface temperature (LST) and land use land cover (LULC) in Bhairab, Kishoreganj, Bangladesh: A geospatial analysis from 2008 to 2023. *Case Studies in Chemical and Environmental Engineering*, 9, 100560.
- [4] Gupta, S.K., Kanga, S., Meraj, G. et al. Optimizing land use for climate mitigation using nature-based solution (NBS) strategy: a study on afforestation potential and carbon sequestration in Rajasthan, India. *Discov Geosci* 2, 36 (2024).
- [5] Y Tarazona, F Benitez-Paez, J Nowosad, F Drenkhan, M. Timana, " scikit-eo: A Python package for Remote Sensing Data Analysis" 2023, *Journal of Open-Source Software*.
- [6] N Kulkarni, H Pande, P Tiwari, S Agrawal "Urban Features Extraction from High Resolution Satellite Image using DL-based semantic segmentation algorithms" 2020, *IIRS - ISRO*.
- [7] F Nurnalisa, E Meilianda, Azmeri "Analysis of land use change using NDVI as input parameter for flood risk assessment of Krueng Kluet watershed in South Aceh, Indonesia" 2022, *E3S Web of Conferences*.
- [8] H Tamiminiaa , B Salehia , M. Mahdianparib, L. Quackenbusha , S. Adelia and B. Briscoe "Google Earth Engine for geobig data applications: A meta-analysis and systematic review." *ISPRS Journal of Photogrammetry and Remote Sensing* Volume 164, June 2020. <https://doi.org/10.1016/j.isprsjprs.2020.04.001>
- [9] A. Nallapareddy "Detection and classification of vegetation areas from red and near infrared bands of Landsat - 8 Optical Image Satellite." *Applied Computer Science*, vol. 18, 2022.
- [10] Kiwelekar A.W., Mahamunkar G.S., Netak L.D., Nikam V.B. (2020) Deep Learning Techniques for Geospatial Data Analysis. In: Tsihrintzis G., Jain L. (eds) *Machine Learning Paradigms. Learning and Analytics in Intelligent Systems*, vol 18. Springer, Cham. [https://doi.org/10.1007/978-3-030-49724-8\\_3](https://doi.org/10.1007/978-3-030-49724-8_3)
- [11] Momm, H., & Easson, G. (2011). Feature Extraction from HighResolution Remotely Sensed Imagery using Evolutionary Computation. In E. Kita (Ed.), *Evolutionary Algorithms*. IntechOpen.
- [12] M. Seyam, M. A. Haque, and M. S. Rahman, "Identifying the land use land cover (LULC) changes using remote sensing and GIS approach: A case study at Bhaluka in Mymensingh, Bangladesh," *Case Studies in Chemical and Environmental Engineering*, vol. 19, no. 4, pp. 100-110, 2023
- [13] H. Wang, X. Liu, C. Zhao, Y. Chang, Y. Liu and F Zang, "Spatialtemporal pattern analysis of landscape ecological risk assessment based on land use/land cover change in Baishuijiang National nature reserve in Gansu Province, China" *Ecological Indicators*, vol. 124, May 2021, 107454
- [14] Amini, S.; Saber, M.; Rabiei-Dastjerdi, H.; Homayouni, S. Urban Land Use and Land Cover Change Analysis Using Random Forest Classification of Landsat Time Series. *Remote Sens.* 2022, 14, 2654
- [15] L. Parra, "Remote Sensing and GIS in Environmental Monitoring." *MDPI Appl. Sci.* 2022, 12, 8045.
- [16] B. Srivastava, "Application of Remote Sensing and GIS in Land Resource Management and Planning " *IJCRT* Volume 11, Issue 5 May 2023.
- [17] M. Digra, R. Dhir and N. Sharma, "Land use land cover classification of remote sensing images based on the deep learning approaches: a statistical analysis and review." *Arabian Journal of Geosciences* (2022) 15:1003
- [18] S. Ullah, X. Qiao M. Abbas "Addressing the impact of land use land cover changes on land surface temperature using machine learning algorithms" *Scientific Reports* (2024) 14:18746
- [19] P. Kempeneers, O Pesek, D. Marchi and P. Soille "pyjeo: A Python Package for the Analysis of Geospatial Data" *SPRS Int. J. Geo-Inf.* 2019, 8(10), 461; <https://doi.org/10.3390/ijgi8100461>
- [20] K. Adepoju and S. Adelabu "Improving accuracy of Landsat-8 OLI classification using image composite and multisource data with Google Earth Engine." 2020, *Remote Sensing Letters* 11(2):107-116